Desalination and Water Treatment
www.deswater.com
doi: 10.1080/19443994.2015.1014859

57 (2016) 7085–7097
March

Taylor & Francis
Taylor & Francis Group

Kinetic and equilibrium study of methylene blue adsorption using H_2SO_4− activated rice husk ash

Gül Kaykioğlu, Elçin Güneş*

Corlu Engineering Faculty, Department of Environmental Engineering, Namik Kemal University, 59860, Corlu-Tekirdag, Turkey, Tel. +90 282 250 2369; Fax: +90 282 652 9372; email: gkaykioglu@nku.edu.tr (G. Kaykioğlu), Tel. +90 282 250 2341, Fax: +90 282 652 9372; email: egunes@nku.edu.tr (E. Güneş)

Received 11 June 2014; Accepted 26 January 2015

ABSTRACT

The objective of this study is to evaluate the performance of H_2SO_4− activated rice husk ash (ARHA) (burned at different temperatures (300–550˚C) as compared to granular activated carbon (GAC) in the removal of methylene blue (MB) from aqueous solution. Batch studies were performed to evaluate the influences of various experimental parameters like pH (4, 7, 9, and 11), initial concentration (5, 10, 15, 20, 25, and 50 mg/L), and contact time (0, 1, 5, 15, 30, 45, 60, 90, and 120 min). BET surface areas for ARHA300 (burned at 300˚C) and ARHA550 (burned at 550˚C) were determined as 143 and 68 m^2/g, respectively. It was observed that the dye uptake by GAC and ARHA300 were not changed significantly when the pH of dye solution was increased from 4 to 11. Uptakes of dye were rapid and the adsorption increased with increasing contact time in all experiments. According to the R^2 values for the adsorption of MB on ARHA300, ARHA500, and GAC, Langmuir model yields fit better than the Freundlich model. The maximum adsorption capacity, q_{max} of ARHA300 (44.25 mg/g), had the highest value. The pseudo-second-order kinetic model yields the best fit for adsorption on ARHA300 and ARHA550 and the correlation coefficients R^2 of the model for the linear plots are very close to 1 at various concentrations.

Keywords: Adsorption; Activated rice husk ash; Activated carbon; MB; Color removal

1. Introduction

Most industries such as textiles, pulp mills, leather, dye synthesis, printing, food, and plastics use dyes and pigments to color their products. Discharge of dye-bearing wastewater into natural streams from industries poses a severe problem. Nowadays, especially in areas which have intensive industrial wastewater discharges, receiving water flows have become colorful and pollution has reached to disturbing levels. In addition to the aesthetic importance of the color parameter, it has negative impacts such as reducing the light transmittance and affecting aquatic organisms' lives [1]. Recently, the color parameter is one of the important parameters for industrial wastewater treatment. Demand for reuse of treated wastewater and restriction of discharge standards have caused increase the need for color removal. In Turkey, as a result of adding color discharge standard to the Water Pollution Control Regulation, evaluation of color removal is necessary and studies which are focused on color removal have increased.

*Corresponding author.

There are many conventional methods for color removal such as oxidation, ion exchange, activated carbon adsorption, membrane technology, and coagulation [2]. Adsorption process is one of the most effective methods for color removal. Although, activated carbon is undoubtedly considered as universal adsorbent for the removal of diverse kinds of pollutants from water [2]. Activated carbon is a highly porous material and has large adsorption capacity [3]. Its widespread use is sometimes restricted due to the high costs and attempts which have been made from different materials to develop low-cost alternative adsorbents such as organic materials, inorganic materials, natural materials, synthesized products, and industrial and agricultural wastes. Activated carbon can be obtained from carbon-rich source of organic materials [4]. Agricultural wastes are the most important source of activated carbon. The agricultural solid wastes are cheap and readily available resources such as almond shell, hazelnut shell, poplar, walnut sawdust [5], orange peel [6,7], sawdust [8], rice husk [9], sugarcane bagasse [10], coconut burch waste [11], and tea leaves [12]. They have been investigated to remove pollutants from aqueous solutions. The various activation procedures are generally applied to improve the specific surface areas of obtained active carbons from agricultural wastes.

Rice is cultivated in more than 75 countries in the world [13] and developing countries around the world produce 500 million tons of rice annually. In Turkey, the estimated production of rice amount is 750 000 tons yearly [14]. Furthermore, about 50% of rice production in Turkey is produced in Edirne province where is in Maritsa basin (372 000 ton/year) and approximately 70 000 tons of this value is rice husk. This causes some problems which occur due to the increase in the amount of rice husk [14]. Therefore, investigation of beneficial uses of rice husk is a very interesting topic. Rice husk is an agricultural residue containing organic materials (lignin, carbohydrates, cellulose, etc.) and inorganic component (about 10% of silica) [15]. Rice husk ash contains approximately 99 wt% silica [3]. In Turkey, rice husk is an abundantly available agricultural waste and can be used as a low-cost adsorbent to remove contaminants in effluent streams. So, large volume of rice husk as agricultural waste can be partly reduced and converted to be used beneficially as low-cost adsorbents for wastewater treatment [16]. Many researchers have studied to removal of color from aqueous solution by rice husk as adsorbent [2,17–21].

In this paper, rice husk ashes (300 and 550˚C burned) named as RHA300 and RHA550 were treated with sulfuric acid to produce adsorbents named as activated rice husk ashes (ARHA300) and the activated rice husk ashes (ARHA550). The capability of produced activated adsorbents by the rice husk burned at different temperatures to remove methylene blue (MB) from aqueous solution was tested by comparing it with granular activated carbon (GAC) and removal mechanism was investigated. The effects of pH, initial dye concentration, and contact time on the adsorption of produced adsorbents were investigated using batch experiments.

2. Materials and Methods

2.1. Preparation of adsorbents

The rice husk which has been used in the study was obtained from a rice processing factory in the district of Edirne province Uzunköprü, Turkey. Raw rice husks were washed with a stream of distilled water to remove dirt, dust, and superficial impurities and then dried in an oven at 105˚C for 24 h. Rice husks were carbonized in air in a muffle furnace at 300˚C for 45 min (RHA300) and 550˚C for 30 min (RHA550), and cooled to room temperature.

The rice husk ashes in a 1:1 wt ratio with 98% H_2SO_4 were soaked for 24 h at room temperature. The acid applied rice husk ashes were heated to 120˚C in an oven for 24 h. After this, the samples were cooled to room temperature, washed with distilled water, and soaked in 1% $NaHCO_3$ solution to remove any remaining acid. After that, the ashes were washed again with distilled water until pH ~6. The activated rice husk ashes (ARHA300 and ARHA550) were dried at 105˚C for 5 h [19].

2.2. Dye sorption

MB is a cationic dye and is used abundantly in the textile industry and paper industry [19]. The structural formula of the MB is given in Fig. 1. MB supplied by Merck was used as an adsorbate. A stock solution of MB dye was prepared (500 mg/L) by dissolving the required amount of dye powder in distilled water. The stock solution was diluted with distilled water to obtain desired concentration ranging from 5 to 50 mg/L.

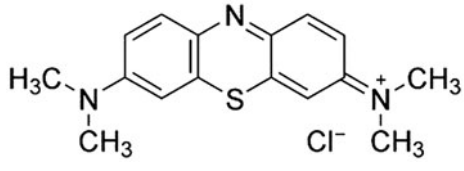

Fig. 1. Molecular structure of MB.

Adsorption studies were carried out at 25°C under batch mode using a orbital shaker at constant agitating speed of 200 rpm. The effect of contact time (0, 1, 5, 15, 30, 45, 60, 90, and 120 min), initial dye concentration (5, 10, 15, 20, 25, and 50 mg/L), and pH (4, 7, 9, and 11) on color removal were studied in a series of kinetic and equilibrium experiments. Adsorbent dose was 1 g/L. The samples were taken from supernatant after contact time and centrifuged (CN180 Nüvefuge) at 3,500 rpm for 5 min and absorbance of MB was measured. The pH of the solution was adjusted using either 0.1 N NaOH or 0.1 N HCl.

2.3. Analysis

Multipoint BET surface area analysis of adsorbent samples was carried out using Quantachrome Instruments brand Nova 4000E model surface area equipment. Pre-preparation stage for samples was heated at 150°C for 16 h in oven. After this, samples were dried under nitrogen gas at 300°C for 5 h in gassing part of the device.

Semi-quantitative elemental analysis was determined using Philips PW-2404 model X-ray fluorescence spectrometer with wavelength dispersive.

Scanned electron microscope (SEM) examination and particle size analysis were determined using JEOL/JSM-6335F-INCA/EDS (scanned electron microscope) and Mastersizer 2000 with laser light scattering technique, respectively. The average grain size results of particle size analysis are 814.292 and 148.277 μm for ARHA300 and ARHA550, respectively.

The adsorption of MB from aqueous solution onto ARHA300 and ARHA550 and GAC was performed using batch experiments in this study.

The residual concentration of the dye was determined using a calibration curve prepared at the corresponding maximum wavelength of 670 nm using a Thermospectronic Aquamate Spectrometer. Results were analyzed using linear Langmuir and Freundlich isotherms.

3. Results

3.1. Characteristics of adsorbents

The color of burned rice husk ash at 300°C is black and at 550°C is gray. The chemical composition of adsorbents and the results of BET surface area analysis are given in Tables 1 and 2, respectively.

According to Table 2, spesific surface area (BET) of used GAC in this study has a high value as 825 m^2/g. BET for ARHA300 and ARHA550 are 143 and 68 m^2/g, respectively. Combustion at high temperature reduced the surface area instead of increasing it. Chandrasekhar and Pramada [20] compared the surface areas of different temperatures as a result of burning in their study. They claim that rice husks were used for two kinds of very different surface areas depending on the temperature (KRH300:11.38 m^2/g, KRH500: 101.29 m^2/g ve APRH300: 25.07 m^2/g, APRH500:14.38 m^2/g).

Table 1
Chemical composition analysis of the rice husk ashes (300 and 550°C)

Element (%)	The ARHA (300°C)	The ARHA (550°C)
Al	0.028	0.026
Ca	0.032	0.075
Cl	–	0.051
Cr	0.006	0.010
Fe	0.045	0.060
K	0.223	0.524
Mg	0.033	0.097
Mn	0.006	0.020
Mo	0.006	0.002
Na	1.362	0.213
O	53.006	52.910
P	0.028	0.015
S	2.920	0.423
Si	41.99	45.565
Zn	0.0223	0.010
Ti	0.011	–

Table 2
BET surface areas of adsorbents

Adsorbent	BET surface area (m^2/g)
ARHA300	143
ARHA550	68
GAC	825

The main functional groups in ash are carbonyl groups which decrease with increasing combustion temperature. The situation contributes to the reduction of surface hydroxyl groups [20]. The surface area of rice husk ash depends on produced amorphous carbon and silica during combustion.

According to the morphological assessment based on SEM images, GAC has a highly prous structure that is supported by the result of BET surface area. SEM images of adsorbents are shown in Fig. 2. Before the heat treatment procedures, raw rice husk looks like a corncob. Rice husk has a regular, circular, and dented structure. After a procedure at 300°C, rice husk ash (RHA300) isn't completely burned and rice husk structure isn't totally ruined [20]. After burning, the circular structure of rice husk became prominent. The activation method made a prominent change in

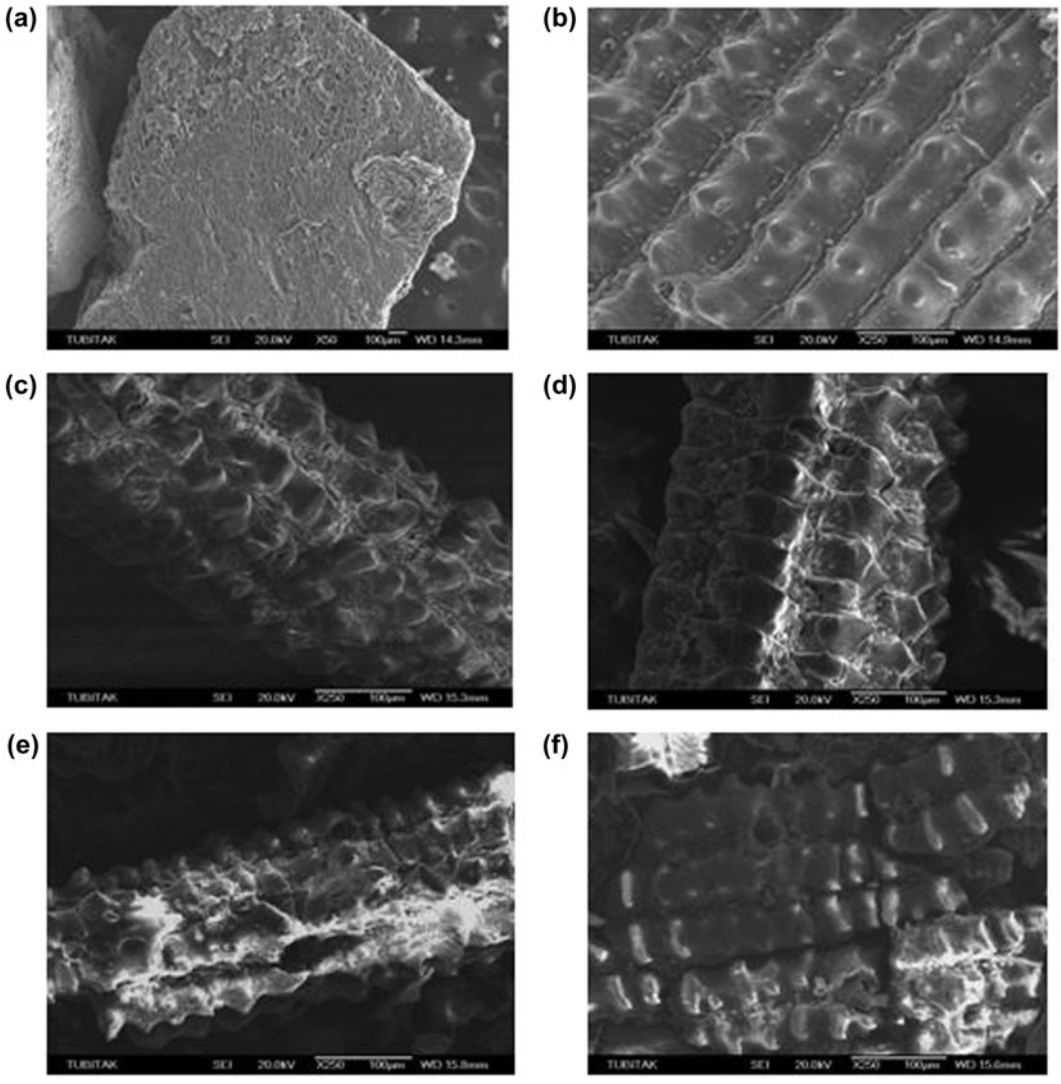

Fig. 2. SEM images of adsorbents: (a) GAC; (b) raw rice husk; (c) RHA300; (d) ARHA300; (e) RHA550; (f) ARHA550.

morphology for ARHA300. Rice husk burnt at 550˚C (RHA550), was mostly damaged, the structural frame was partially remained, big holes were formed and the regular structure was destroyed. According to a recent research by Liou and Wo [3], after a procedure over 500˚C, the surface area and adsoption capacities decreased and the microporouse structure which formed at lower temperatures was ruined. The activation method used for rice husk burnt at 550˚C (ARHA550) did not make a prominent effect on the change of morphology.

3.2. Effect of pH

The pH of solution which is an important controlling parameter in the adsorption process affects the surface charge of the adsorbents and the adsorption capacity. The dye adsorption capacity of ARHA300, ARHA550, and GAC are shown in Fig. 3 as a function of pH. In order to assess the effect of pH (4, 7, 9, and 11) on adsorption of dye by ARHA300, ARHA550, and GAC, similar experiments were performed at C_0 = 20 mg/L dye concentration. It was observed that the dye uptake by GAC and ARHA300 did not change significantly. However, when the pH of dye solution was increased from 4 to 11, dye adsorption by GAC and ARHA300 at equilibrium slightly increased from 12.09 to 12.84 mg/g and decreased from 17.55 to 17.21 mg/g, respectively. In addition, the dye adsorption by ARHA550 with increased pH gradually increased from 4.63 to 16.83 mg/g. It is a common observation that the surface adsorbs anions favorably

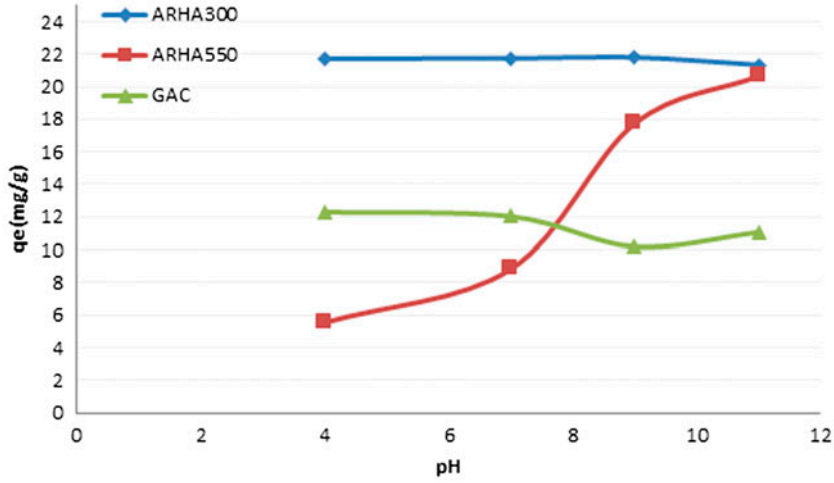

Fig. 3. Effect of pH on dye adsorption.

at lower pH due to presence of H^+ ions, whereas, the surface is active for the adsorption of cations at higher pH due to the deposition of OH^- ions. Lower adsorption of ARHA550 at acidic pH is provable owing to the presence of excess of H^+ ions competing with the dye cations for the adsorption sites. The maximum dye removal by ARHA550 was observed at pH 11.

The point of zero charge (pH_{PZC}) of the adsorbent is necessary to determine the adsorption mechanism. Adsorption of cations is favored at $pH > pH_{PZC}$. The pH_{pzc} of ARHA300 and ARHA550 were found to be 10.2 using zeta potential meter. Surfaces of the ARHA300 and ARHA550 are positively charged for pH values below 10.2. In this case, when the pH value was higher than pH_{pzc}, the surface of ARHA300 and ARHA550 became negatively charged and the adsorption of positively charged MB was enhanced though electrostatic force attraction. For ARHA300 and GAC, electrostatic force attraction can not fully explain with almost constantly of adsorption capacity from 4 to 11. It is possible that ion exchange was involved in the adsorption process. As silica is one of the most important constituents of rice hull ash, the adsorption of dyes can take place by the cation exchange reaction through the substitution of protons from silanol groups on the surface with cations of dye from the solution [22].

Hydrogen bonds are presumed to form between the OH^- and O^- groups on the surface of silica and the amino groups of dye molecules. Rice husk ash contains OH^- groups on the surface therefore it is negative. And for this reason, it has high adsorption capacity for cationic dyes [20]. After a high-temperatured procedure over 700˚C on the surface of carbon atoms, a basic character is formed within the carbon surface and if the applied temperature increases, the OH^- groups seem to decrease [20]. When pH is bigger than 7, the surface has a negative charge [20]. This situation may change physical and chemical structures of ARHA300 (ion change only) and ARHA550 (ion exchange and electrostatic affinity) and their adsorption capacities due to pH. During the ion exchange process, the dye moved both through the pores of adsorbent mass and through the channels of lattice. The diffusion was faster through pores and was retarded when the ion moved through the smaller diameter channels [23]. Maximum qe levels are obtained at pH 11, and so, this pH was taken as the reference pH in the following assesments.

3.3. Effect of contact time

The adsorption at equilibrium of MB by GAC, ARHA300, and ARHA550 at 20 mg/L initial concentration and at constant pH (pH 11) are shown in Fig. 4. Uptakes of dye were rapid and the adsorption got higher with increasing contact time. The equilibriums were attained within 120 min for ARHA300, ARHA550. Therefore, the contact time was set to 120 min in each experiment.

3.4. Effect of initial dye concentration

The effect of initial dye concentration on the removal of MB by ARHA300, ARHA550, and GAC is shown in Figs. 5 and 6. The removal efficiency (q_e) of MB by ARHA300, ARHA550, and GAC increased from 3.96 to 41.55 mg/g, 4.07 to 29.03 mg/g, and 4.02 to 12.00 mg/g by increasing dye concentration (from 5 to 50 mg/L), respectively.

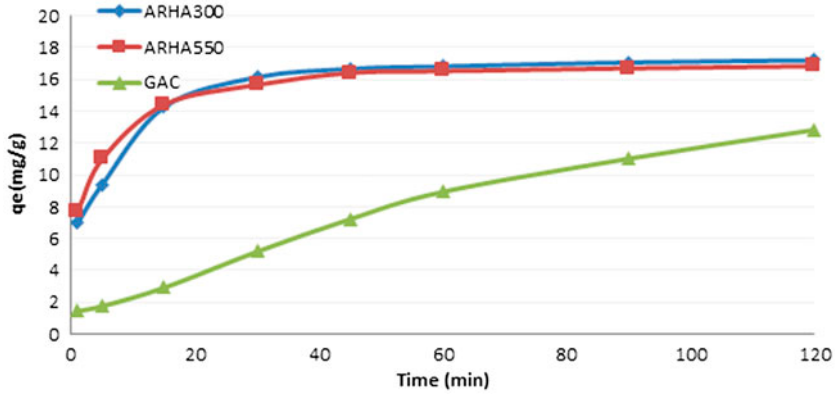

Fig. 4. Effect of contact time on dye adsorption.

The initial dye concentration provides the necessary driving force to overcome the resistances of the mass transfer of MB between the aqueous and the solid phases [21]. So, increase of initial dye concentration will increase the driving force and adsorption rate [24]. Whereas, the percentage MB adsorption at equilibrium decreased from 86 to 52% for ARHA550 and from 85 to 4% for GAC, it is increased from 83 to 88% for ARHA300. For ARHA300, the percentage MB adsorption at equilibrium constant was at nearly 90% for initial dye concentration from 10 to 50 mg/L and was not a significant decrease for ARHA550 and GAC. Generally, the extent of the dye removal was found to be strongly dependent on the concentration of dye. The increase in initial dye concentration enhances the interaction between MB and adsorbents. Therefore, an increase in initial dye concentration of MB enhances the adsorption of MB. The rate of adsorption also gets higher with the increase in initial dye concentration due to increase in the driving force of ARHA300.

At lower initial concentrations, dye in solution interacts with the binding sites and, thus, higher adsorption rate was obtained for GAC and ARHA550. In contrast, at higher initial concentrations, due to the saturation of binding sites, adsorption rate decreased. This is due to energetically less favorable sites becoming involved with increasing dye concentration in solution [23,25].

3.5. Adsorption equilibrium study

For adsorption studies, it is important to establish the most appropriate correlation for the equilibrium curves in order to optimize the design of an adsorption system. Several isotherm models like Freundlich, Langmuir, R–P, Temkin, and D–R have been used to describe the equilibrium characteristics of adsorption

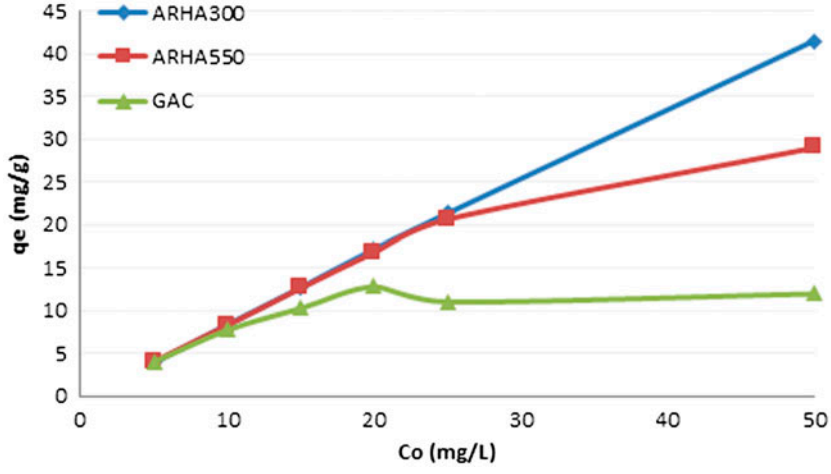

Fig. 5. Effect to adsorption rate of initial dye concentration on dye adsorption.

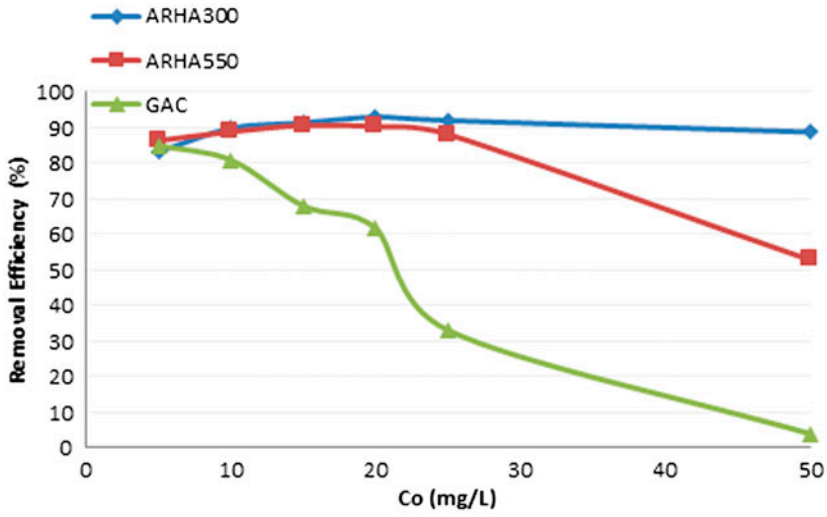

Fig. 6. Effect to removal efficiency (q_e) of initial dye concentration.

[21]. In this study, the Langmuir and Freundlich adsorption isoterms were employed.

The Langmuir equation is used to estimate the maximum adsorption capacity corresponding to complete monolayer coverage on the adsorbent surface and is expressed as follows [19]:

$$q_e = \frac{(q_{\max} K_L C_e)}{(1 + K_L C_e)} \tag{1}$$

where q_e (mg/g) is the amount of MB adsorbed per unit mass of adsorbent particles at equilibrium, and C_e (mg/L) is the equilibrium liquid concentration of MB; K_L is the equilibrium constant (L/mg), and $q_{\max}$ is the amount of adsorbate required to form monolayer (mg/g) [26].

The linearized equation of Langmuir is represented as follows:

$$\frac{C_e}{q_e} = \frac{1}{q_{\max} K_L} + \frac{C_e}{q_{\max}} \tag{2}$$

The experimental data is then fitted into the above equation for linearization by plotting C_e/q_e against C_e [19].

The Freundlich model is an empirical equation used to estimate the adsorption intensity of the sorbent towards the adsorbate. The Freundlich model and the linearized equation of Freundlich are given below [19]:

$$q_e = K_f C_e \frac{1}{n} \tag{3}$$

$$\ln q_e = \ln K_f + \frac{1}{n} \ln C_e \tag{4}$$

If a plot of ln C_e against ln q_e yielding a straight line it indicates the adaptation of the Freundlich model. The value of n indicates the affinity of the adsorbate toward the adsorbent. $1/n$ and K_f can be calculated from the slope and intercept, respectively [19].

Figs. 7 and 8 present Langmuir and Freundlich isotherm plots for the adsorption of MB on ARHA300, ARHA500, and GAC. Table 3 gives the $q_{\max}$ and K_L values for Langmuir isotherm, K_f and n values for the Freundlich isotherm and the correlation coefficients for the two isotherms. It can be seen from the R^2 values in Figs. 7, 8, and Table 3 that Langmuir model yields better fit than the Freundlich model for the adsorption of MB on ARHA300, ARHA500, and GAC. So The Langmuir model which based on monolayer, uniform, and finite adsorption site assumptions represent the experimental data well. It can be seen from the Table 3 that the maximum adsorption capacity of ARHA300 which had q_{max} value of 44.25 mg/g had the biggest value. As it can be seen from Table 2 that GAC has the biggest BET surface area but has the smallest q_{max} value of 12.22 mg/g. In literature, it is presented that commonly used activated carbons are microporous materials that are efficient in removing molecules of size smaller than the width of micropores (typically below 2 nm). However, activated carbon is not as efficient in removing dyes which have high molecular weight. This is due to the adsorption equilibrium establishing slowly as a result of low solute diffusion within the internal pores with large molecular weight compounds [27]. In this study, it is

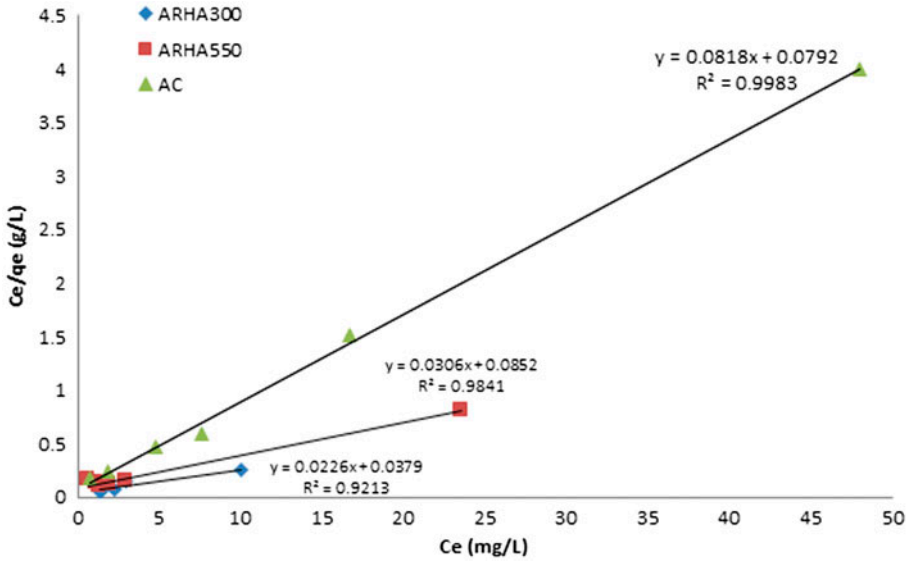

Fig. 7. Langmuir isotherm plots for the adsorption of MB on ARHA300, ARHA500 and GAC (pH = 11, t = 120 min, C_0 = 5, 10, 15, 20, 25, 50 mg/L, m = 1 g/L).

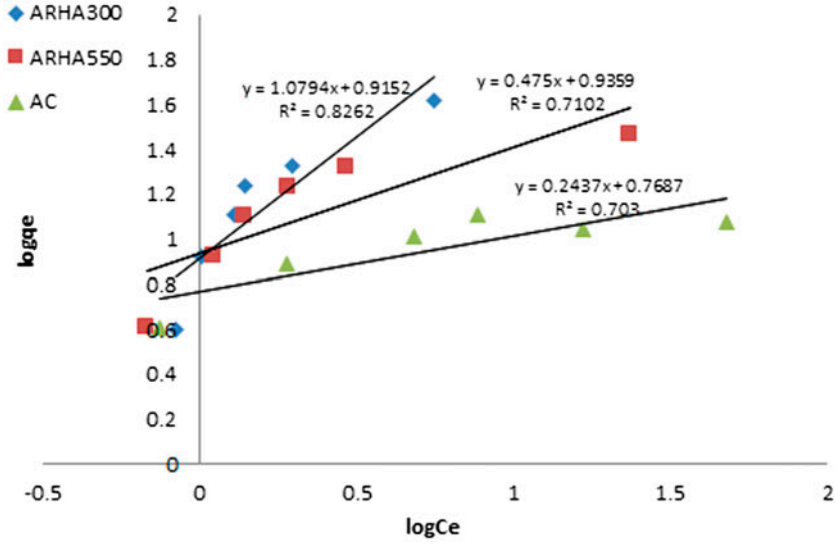

Fig. 8. Freundlich isotherm plots for the adsorption of MB on ARHA300, ARHA500 and GAC (pH = 11, t = 120 min, C_0 = 5, 10, 15, 20, 25, 50 mg/L, m = 1 g/L).

estimated that GAC is not efficient for removing this dye molecules because of pore size.

McKay et al. [28] defined a dimensionless separation factor R_L to explain the essential characteristic of Langmuir equation, as given below [25]:

$$R_L = 1/(1 + K_L C_0) \quad (5)$$

Favorable adsorption is indicated by $0 < R_L < 1$ [23]. The R_L values were found to be between 0 and 1 for dye concentrations between 5 and 50 mg/L for ARHA300, ARHA550, and GAC (Data are not shown in Table 3). So, it can be concluded from the R_L values that favorable adsorption of MB existed on ARHA300, ARHA550, and GAC.

Table 3
Isotherm constants for the Langmuir and Freundlich isotherms

	Langmuir isotherm			Freundlich isotherm		
Adsorbent	q_{max} (mg/g)	K_L (L/g)	R^2	K_f	$1/n$	R^2
ARHA300	44.25	0.596	0.9213	7.95	1.28	0.9045
ARHA550	32.68	0.369	0.9841	8.21	0.66	0.8905
GAC	12.22	1.033	0.9983	5.20	0.38	0.9002

K_f and $1/n$ values in Freundlich isotherm model indicate the adsorption capacity and adsorption intensity, respectively. The higher the value of $1/n$, the higher will be the affinity and the heterogenity of the adsorbent sites. Values of $1/n < 1$ show the favorable nature of adsorption of MB on the adsorbents [21]. As it can be seen from the Table 3 that MB adsorption on ARHA550 and GAC have $1/n$ values 0.66 and 0.38, respectively. This result showed the favorable nature of adsorption of MB on these adsorbents and the higher value of $1/n$ of ARHA550 ($1/n = 0.66$) showed the affinty and heterogenity of adsorbent sites.

3.6. Adsorption kinetic study

One of the most important factors in evaluating the efficiency of sorption is analyzing the rate of the sorption [29,30]. So, we conducted experiments to assess the kinetics of MB removal on ARHA300, ARHA550, and GAC. In the kinetics experiments, the adsorption reached equilibrium after 120 min as no significant increase in MB adsorption was observed after that time. Kinetics of MB adsorption on the adsorbents was analyzed using pseudo-first-order, pseudo-second-order, and Elovich models.

The lagergren equation is probably the earliest known example describing the rate of adsorption in the liquid-phase systems. This equation has been one of the most used equations for pseudo-first-order kinetics and expressed as follows [31]:

$$\frac{dq_t}{dt} = k_1(q_e - q_t) \tag{6}$$

In this equation, k_1 is the pseudo-first-order adsorption rate coefficient (min^{-1}), q_e is the amount adsorbed (mg/g) at equilibrium, q_t is the amount adsorbed (mg/g) at time t. The integrated form of Eq. (6) for the boundary conditions of $t = 0$, $q_t = 0$ and $t = t$, $q_t = q_t$,

$$(\log q_e - \log q_t) = \log q_e - \frac{k_1}{2.303}t \tag{7}$$

The straight line of the plot of $\log(q_e–q_t)$ vs. t show the applicability of the pseudo-first-order equation for the system [26]. The values of q_e, calculated and k_1 can be determined from the slope and intercept of the plots.

The pseudo-second-order adsorption kinetic rate equation and integrated form of the equation for boundary conditions $t = 0 – t = t$ and $q_t = 0 – q_t = q_t$ is expressed as follows [19]:

$$\frac{dq_t}{dt} = k_2(q_e - q_t)^2 \tag{8}$$

$$\frac{1}{(q_e - q_t)} = \frac{1}{q_e} + kt \tag{9}$$

$$\frac{1}{q_t} = \frac{1}{k_2 q_e^2} + \frac{1}{q_e}t \tag{10}$$

If the initial adsorption rate, h (mg/g min) is as follows, then Eq. (10) will become as in Eq. (12):

$$h = k_2 q_e^2 \tag{11}$$

$$\frac{t}{q_t} = \frac{1}{h} + \frac{1}{q_e}t \tag{12}$$

The straight line of the plot (t/q_t) of vs. t shows the applicability of the pseudo-first-order equation for the system. Then q_e and k_2 can be determined from the slope and intercept of the plot.

The Elovich model is generally expressed as follows [19]:

$$\frac{dq_t}{dt} = \alpha \exp(-\beta q_t) \tag{13}$$

The simplified Elovich equation for boundary conditions $t = 0 – t = t$ and $q_t = 0 – q_t = q_t$ is as follows [19]:

$$q_t = \frac{1}{\beta}\ln(\alpha\beta) + \frac{1}{\beta}\ln(t) \tag{14}$$

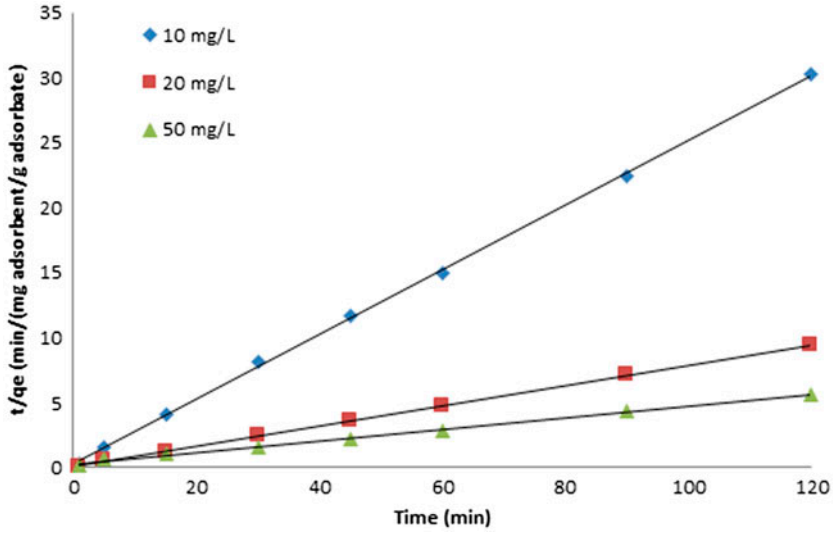

Fig. 9. Plot of pseudo second-order equation for adsorption of MB on ARHA300 at different initial concentrations (pH = 11, t = 120 min, C_0 = 10, 20, 50 mg/L, m = 1 g/L).

It is postulated that the Elovich coefficients, α and $ß$, represent the initial adsorption rate (mg/g min) and the desorption coefficient (mg/g min), respectively. If the adsorption system fits this model, a plot of q_t vs. ln(t) should yield linear relationship with a slope of (1/β) and an intercept of (1/β) ln($\alpha\beta$) [19,31].

As it is known, a relatively high correlation coefficient (R^2, close or equal to 1) value indicates that the model successfully describes the kinetics of adsorption system. As it is seen from the Figs. 9, 10, and Table 4 for MB adsorption on ARHA300 and ARHA550, the pseudo-second-order kinetic model yielded the best fit and the correlation coefficients R^2 of the model for the linear plots were very close to 1 at various concentrations. So as R^2 values considered, it was found that the adsorption rates of MB using ARHA300 and ARHA550 fit to pseudo-second-order kinetic model well. In many studies, it was indicated that the value of k_2 usually depends on the initial adsorbate concentration in the bulk phase. The rate coefficient, k_2, decreases with the increasing initial adsorbate concentration as a rule, where k_2 is interpreted as a time-scaling factor. Thus, higher is the initial concentration of adsorbate, the longer time is required to

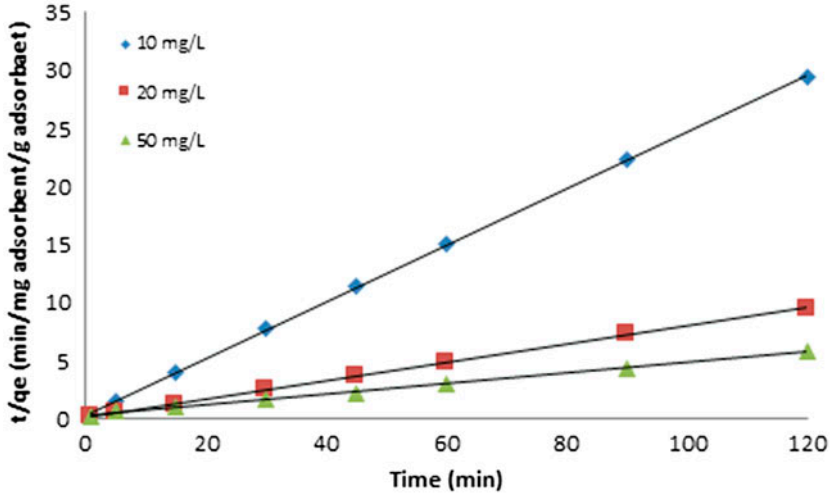

Fig. 10. Plot of pseudo second-order equation for adsorption of MB on ARHA550 at different initial concentrations (pH = 11, t = 120 min, C_0 = 10, 20, 50 mg/L, m = 1 g/L).

Table 4
Kinetic parameters for the removal of MB by ARHA300, ARHA550, and AC (t = 120 min, C_0 = 10, 20, 50 mg/L, m = 1 g/L, pH = 11)

ARHA300				
C_0 (mg/L)	q_e,exp (mg/g)	q_e,calc (mg/g)	k_f (min^{-1})	R^2
Pseudo-first-order model				
10	8.388	1.396	0.0467	0.9317
20	17.215	7.281	0.0483	0.9468
50	41.553	59.347	0.0665	0.9588
Pseudo-second-order model				
C_0 (mg/L)	q_e,calc (mg/g)	h (g/mg min)	k_s (g/mg min)	R^2
10	4.022	3.054	0.189	0.9995
20	12.820	12.936	0.078	0.9999
50	22.472	3.879	0.0076	0.9971
Elovich model				
C_0 (mg/L)		β	α	R^2
10		2.320	$15*10^5$	0.8782
20		0.422	44.330	0.9457
50		0.099	5.509	0.8377
ARHA550				
Pseudo-first-order model				
C_0 (mg/L)	q_e,exp (mg/g)	q_e,calc (mg/g)	k_f (min^{-1})	R^2
10	8.317	1.909	0.0605	0.9549
20	16.842	6.046	0.0472	0.9411
50	29.031	32.951	0.0246	0.9671
Pseudo-second-order model				
C_0 (mg/L)	q_e,calc (mg/g)	h (g/mg min)	k_s (g/mg min)	R^2
10	4.100	2.693	0.160	0.9998
20	12.723	8.305	0.051	0.9998
50	22.075	3.037	0.006	0.9979
Elovich model				
C_0 (mg/L)		β	α	R^2
10		1.841	34,886	0.9295
20		0.495	112.69	0.9611
50		0.1690	2.85	0.7953
GAC				
Pseudo-first-order model				
C_0 (mg/L)	q_e,exp (mg/g)	q_e,calc (mg/g)	k_f (min^{-1})	R^2
10	7.761	6.945	0.0248	0.9816
20	12.842	12.968	0.0207	0.9828
50	12.001	11.606	0.0186	0.9882
Pseudo-second-order model				
C_0 (mg/L)	q_e,calc (mg/g)	h (g/mg min)	k_s (g/mg min)	R^2
10	4.188	0.414	0.0236	0.9800
20	11.482	0.613	0.0046	0.9401
50	16.861	0.225	0.0007	0.6639
Elovich model				
C_0 (mg/L)		β	α	R^2
10		0.837	2.690	0.6630
20		0.419	1.569	0.8028
50		0.466	1.547	0.8022

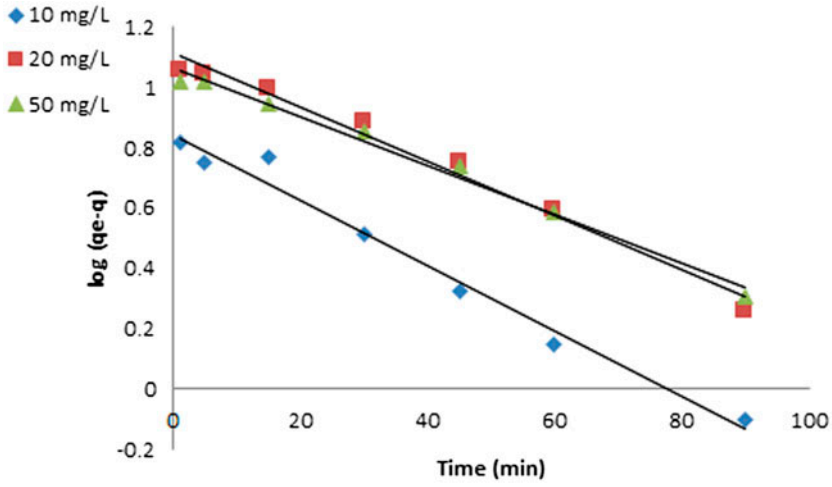

Fig. 11. Plot of pseudo first-order equation for adsorption of MB on AC at different initial concentrations (pH = 11, t = 120 min, C_0 = 10, 20, 50 mg/L, m = 1 g/L).

reach an equilibrium, in turn, the k_2 value decreases [31]. Also in this study, it was found that k_2 values decreased with increasing initial concentration for ARHA300 and ARHA550.

The adsorption rate of MB on GAC was found to fit pseudo-first-order kinetic model. The value of k_1 also depends on the initial concentration of the adsorbate that varies from one system to another. It usually decreases with the increasing initial adsorbate concentration in the bulk phase [31]. As it is seen from Table 4 that for MB adsorption on GAC k_1 decreases with increasing initial MB concentration.

The rate constants and R^2 values and plots of the kinetic models are given in Table 4 and Figs. 9–11.

4. Conclusion

The following conclusions can be drawn based on investigated of MB removal by different burned and chemical-activated rice husk ash (ARHA300 and ARHA550) and GAC.

(1) BET for ARHA300 and ARHA550 were 143 and 68 m^2/g, respectively. The surface area decreased in burned rice husk ash at higher temperature.
(2) It was observed that the dye uptake by GAC and ARHA300 was not changed significantly when the pH of dye solution was increased from 4 to 11. However, lower adsorption of ARHA550 at acidic pH is provable due to the presence of excess of H^+ ions competing with the dye cations for the adsorption sites. The maximum dye removal by ARHA550 was observed at pH 11.
(3) Uptakes of dye were rapid and the adsorption got higher with increasing contact time. The equilibriums were attained within 120 min for ARHA300 and ARHA550.
(4) The rate of adsorption increased with the increase in initial dye concentration due to increase in the driving force for ARHA300. And for GAC and ARHA550 at lower initial concentrations, dye in solution interacted with the binding sites and, thus, higher adsorption rate was obtained.
(5) According to the R^2 values for the adsorption of MB on ARHA300, ARHA500, and GAC, Langmuir model provided better fit than the Freundlich model. The maximum adsorption capacity, q_{max} of ARHA300 which has q_{max} value of 44.25 mg/g had the biggest value.
(6) The adsorption on ARHA300 and ARHA550 the pseudo-second-order kinetic model yielded the best fit and the correlation coefficients R^2 of the model for the linear plots were very close to 1 at various concentrations.

ARHA300 and ARHA550 could be used successfully for removal from synthetic solutions in different concentration and pH values of MB solution which is used as dye stuff with large quantities for textile industry. In the light of the findings, in order to increase of BET surface area and adsorption capacity, more work should be planned with different burning and activation methods.

Acknowledgment

This research was supported by NKU–BAP project no: NKUBAP.00.17.AR.11.01.

References

[1] A.R. Dinçer, Y. Güneş, N. Karakaya, Coal-based bottom ash (CBBA) waste material as adsorbent for removal of textile dyestuffs from aqueous solution, J. Hazard. Mater. 142 (2007) 529–535.
[2] S.T. Ong, C.K. Lee, Z. Zainal, Removal of basic and reactive dyes using ethylenediamine modified rice hull, Bioresour. Technol. 98 (2007) 2792–2799.
[3] T.-H. Liou, S.-J. Wu, Characteristics of microporous/mesoporous carbons prepared from rice husk under base- and acid-treated conditions, J. Hazard. Mater. 171 (2009) 693–703.
[4] D. Kalderis, D. Koutoulakis, P. Paraskeva, E. Diamadopoulos, E. Otal, J.O. del Valle, C. Fern´andez-Pereira, Adsorption of polluting substances on activated carbons prepared from rice husk and sugarcane bagasse, Chem. Eng. 144 (2008) 42–50.
[5] A.H. Aydin, Y. Bulut, O. Yavuz, Acid dyes removal using low cost adsorbents, Int. J. Environ. Pollut. 21 (2004) 97–104.
[6] C. Namasivayam, N. Muniasamy, K. Gayatri, M. Rani, K. Ranganathan, Removal of dyes from aqueous solutions by cellulosic waste orange peel, Bioresour. Technol. 57 (1996) 37–43.
[7] M. Arami, N.Y. Limaee, N.M. Mahmoodi, N.S. Tabrizi, Removal of dyes from colored textile wastewater by orange peel adsorbent: Equilibrium and kinetic studies, J. Colloid Interface Sci. 288 (2005) 371–376.
[8] A. Shukla, Y.-H. Zhang, P. Dubey, J.L. Margrave, S.S. Shukla, The role of sawdust in the removal of unwanted materials from water, J. Hazard. Mater. 95 (2002) 137–152.
[9] V. Vadivelan, K.V. Kumar, Equilibrium, kinetics, mechanism, and process design for the sorption of methylene blue onto rice husk, J. Colloid Interface Sci. 286 (2005) 90–100.
[10] S.C. Ibrahim, M.A.K.M. Hanafiah, M.Z.A. Yahya, Removal of cadmium from aqueous solution by adsorption on sugarcane bagasse, J. Agric. Environ. Sci. 1 (2006) 179–184.
[11] B.H. Hameed, D.K. Mahmoud, A.L. Ahmad, Equilibrium modeling and kinetic studies on the adsorption of basic dye by a low-cost adsorbent: Coconut (*Cocos nucifera*) bunch waste, J. Hazard. Mater. 158 (2008) 65–72.
[12] B.H. Hameed, Spent tea leaves: A new non-conventional and low-cost adsorbent for removal of basic dye from aqueous solutions, J. Hazard. Mater. 161 (2009) 753–759.
[13] E.I. El-Shafey, Removal of Zn(II) and Hg(II) from aqueous solution on a carbonaceous sorbent chemically prepared from rice husk, J. Hazard. Mater. 175 (2010) 319–327.
[14] D. Öztürk, Y.A. Akçay, A general evaluation of rice production in Southern Marmara Region, J. Agric. Faculty Gaziosmanpasa University 27 (2010) 61–70.
[15] J.S. Romano, F.A. Rodrigues, Cements obtained from rice hull: Encapsulation of heavy metals, J. Hazard. Mater. 154 (2008) 1075–1080.
[16] K.Y. Foo, B.H. Hameed, Utilization of rice husk ash as novel adsorbent: A judicious recycling of the colloidal agricultural waste, Adv. Colloid Interface Sci. 152 (2009) 39–47.
[17] D. Sarkar, A. Bandyopadhyay, Adsorptive mass transport of dye on rice husk ash, J. Water Resour. Prot. 2 (2010) 424–431.
[18] A.K. Chowdhury, A.D. Sarkar, A. Bandyopadhyay, Rice husk ash as low cost adsorbent for removal of methylene blue and congo red in aqueous phase, CLEAN—Soil Air Water 37(7) (2009) 581–591.
[19] M.M. El-Halwany, Study of adsorption isotherms and kinetic models for methylene blue adsorption on activated carbon developed from egyptian rice hull (part II), Desalination 250 (2010) 208–213.
[20] S. Chandrasekhar, P.N. Pramada, Rice husk ash as an adsorbent for methylene blue-effect of ashing temperature, Adsorption 12 (2006) 27–43.
[21] V.S. Mane, I.D. Mall, V.C. Srivastava, Kinetic and equilibrium isotherm studies for the adsorptive removal of brilliant green dye from aqueous solution by rice husk ash, J. Environ. Manage. 84 (2007) 390–400.
[22] V.C. Srivastava, I.D. Mall, I.M. Mishra, Characterization of mesoporous rice husk ash (RHA) and adsorption kinetics of metal ions from aqueous solution onto RHA, J. Hazard. Mater. B134 (2006) 257–267.
[23] T.K. Naiya, A.K. Bhattacharyaa, S. Mandal, S.K. Das, The sorption of lead(II) ions on rice husk ash, J. Hazard. Mater. 163 (2009) 1254–1264.
[24] U.R. Lakshmi, V.C. Srivastava, I.D. Mall, D.H. Lataye, Rice husk ash as an effective adsorbent: Evaluation of adsorptive characteristics for Indigo Carmine dye, J. Environ. Manage. 90 (2009) 710–720.
[25] A.R. Dinçer, Y. Güneş, N. Karakaya, E. Güneş, Comparison of activated carbon and bottom ash for removal of reactive dye from aqueous solution, Bioresour. Technol. 98 (2007) 834–839.
[26] H. Aydın, Y. Bulut, Ç. Yerlikaya, Removal og copper (II) from aqueous solution by adsorption onto low-cost adsorbents, J. Environ. Manage. 87 (2008) 37–45.
[27] J. Galán, A. Rodríguez, J.M. Gómez, S.J. Allen, G.M. Walker, Reactive dye adsorption onto a novel mesoporous carbon, Chem. Eng. J. 219 (2013) 62–68.
[28] G. McKay, H. Blair, J.R. Gardiner, The adsorption of dyes onto chitin in fixed bed column and batch adsorbers, J. Appl. Polym. Sci. 28 (1989) 1499–1544.
[29] S. Ayoob, A.K. Gupta, P.B. Bhakat, V.T. Bhat, Investigations on the kinetics and mechanisms of sorptive removal of fluoride from water using alumina cement granules, Chem. Eng. J. 140 (2008) 6–14.
[30] Y.H. Huang, C.L. Hsueh, H.P. Cheng, L.C. Su, C.Y. Chen, Thermodynamics and kinetics of adsorption of Cu(II) onto waste iron oxide, J. Hazard. Mater. 144 (2007) 406–411.
[31] S.S. Gupta, K. Bhattacharyya, Kinetics of adsorption of metal ions on inorganic materials: A review, Adv. Colloid Interface Sci. 162 (2011) 39–58.